

Lanthanide Induced Shifts of Aromatic 1,2,3-Trimethoxy Compounds: Conformational Analysis of Tetrahydrofurofuran-Lignans in Solution

Otmar Hofer and Gerald Wurz

Institute of Organic Chemistry, University of Vienna, A-1090 Wien, Austria

Summary. The solution conformations of 1,4-diaryl-tetrahydro-1*H*,3*H*-furo[3,4-*c*]furans were determined by means of the LIS technique using a modified LIS-simulation program specially designed for the requirements of the aromatic 1,2,3-trimethoxy arrangement as a bidentate coordination site for the NMR shift reagent. The resulting geometries were confirmed by force field calculations (MM2-87) and compared with X-ray derived structures. Reliable data for the conformations in solution allowed a quantitative estimation of the circular dichroism based on the coupled oscillator model.

Keywords. Lanthanide induced shift simulation; Force field; Circular dichroism; Coupled oscillator model; Tetrahydrofurofuran lignans.

Lanthanideninduzierte Verschiebungen von aromatischen 1,2,3-Trimethoxy-Verbindungen: Konformationsanalyse von Tetrahydrofurofuran-Lignanen in Lösung

Zusammenfassung. Es wurden mittels der LIS-Technik die Konformationen von 1,4-Diaryl-tetrahydro-1*H*,3*H*-furo[3,4-*c*]furanen in Lösung bestimmt. Dazu mußte ein modifiziertes LIS-Simulationsprogramm entworfen werden, das auf die besonderen Verhältnisse der aromatischen 1,2,3-Trimethoxy-Gruppierung eingeht, welche in den untersuchten Verbindungen als zweizählige Koordinationsstelle für das NMR-Verschiebungsreagens fungiert. Die resultierenden Geometrien wurden mittels Kraftfeldrechnungen (MM2-87) überprüft und soweit vorhanden auch mit Röntgenstrukturdaten verglichen. Für die Lösungskonformationen wurde eine quantitative Abschätzung des Circular dichroismus auf der Basis des Modells für gekoppelte Oszillatoren durchgeführt.

Introduction

The relative and absolute stereochemistry of 1,4-diaryl-tetrahydro-1*H*,3*H*-furo[3,4-*c*]furans has been subject of several studies [1–10]. Recently the crystal structure of two derivatives, diasartemin (**2**) and episartemin B (**3**), has been established [11]. Since the furofuran lignans have been shown to exhibit some insecticidal [12] and medicinal activities [13], we were interested in the solution structures of these compounds as well.

One of the tools suited for conformational analysis of organic compounds in solution is offered by the lanthanide induced shift method, which was already used

for the proof of the relative stereochemistries [5]. Since most of the derivatives available were characterized by an aromatic trimethoxy arrangement, we designed now a special LIS-simulation program to account for this coordination site. Additional complications are discussed, which are either caused by a 1,2-methylenedioxy-3-methoxy grouping as a second (although weaker) coordination site or by the very special coordination effects due to the 2,5-oxygens of the chair-chair-conformation of the tetrahydrofurofuran system itself. Since neighbouring aromatic methoxy groups are rather often found in natural products and we consider conformational analysis as the ultimate goal of any structure elucidation (e.g. [14, 15]), the knowledge about the complexing behaviour of dimethoxy and trimethoxy towards lanthanide shift reagents should be also of general interest in our further studies on conformational analysis of natural products.

The resulting aryl-conformations (rotation about the tetrahydrofurofuran-phenyl bond) are compared with the results obtained from force field calculations and the X-ray determined geometries in the crystal state. Since the positions of the non-coupled but sterically close aryl chromophors are decisive for sign, line splitting and rotator strength of the CD spectra of these compounds, a quantitative comparison of experimental and calculated CD parameters should provide additional proof of favoured conformations in solution.

Results and Discussion

Computational LIS-Model for 1,2,3-Trimethoxybenzene Derivatives

The model follows the principles applied for 1,2-dimethoxy derivatives as fairly strong bidentate ligands [16]. The possible extension to 1,2,3-trimethoxy compounds has been already indicated in Ref. [16] for 1,2,3-trimethoxybenzene itself. The basic principle is the assumption of two principal magnetic axes for each bidentate coordination site, corresponding to the two lines connecting the oxygen atoms with the coordinated europium ion. In this case of 1,2,3-trimethoxy compounds one may assume a pair of possible bidentately complexing oxygens, the oxygen atom in the middle position (position 2) is involved in both possible complexes.

Due to the steric requirements of the bulky ligands of the shift reagents and the necessary optimal orientation of the free electron orbitals of oxygen in the complexes by rotation about the *MeO*-C(arom.) bond, it is unlikely that two Eu^{3+} ions are complexed at the same time. However, since the complexing equilibria are rapid on the NMR time scale, all possible complexes contribute to the averaged LIS data corresponding to their relative populations. In other words, an averaging of two bidentate coordinations should be well suited to simulate the experimental LIS data of 1,2,3-trimethoxy compounds. This amounts to four magnetic axes to be considered in the calculation. However, a practical use of the principles outlined above was not possible without extensive modifications of the LIS standard program PDIGM [17, 18] used also in Ref. [16].

Therefore, a new, specially designed program was written: (i) to allow double bidentate complexation at 1,2,3-trimethoxy, (ii) to apply optionally a correction due to a second (weaker) coordination site which adds to the dominant coordination at the trimethoxy site, and (iii) to allow an efficient conformational analysis by rotating atom groups of a molecule about particular single bonds.

The latter (iii) was accomplished by the use of an optional geometry input using internal coordinates (construction of the molecule from bond length, bond angles and torsional angles, like in programs of the COORD type [19]), the two former problems (i, ii) were solved by the automatic creation of one complete set of (Cartesian) proton positions for each principal magnetic axis to be considered in the computation.

In other words, *one* molecular geometry is given in the input *either* by cartesian *or* internal coordinates, and then *for every possible principal magnetic axis* (defined by the variable lanthanide ion position and corresponding coordination sites) a transformation of coordinates takes place to arrange the molecule in the usual manner within the Cartesian coordinate system: the coordinating oxygen atom is put into the origin of the coordinate system, the next (aromatic) C along the negative z -axis, and a neighbouring C in the x/z plane. This procedure is now repeated for all n possible principal magnetic axes defined in the input. This results in n sets of coordinates for the proton positions with known experimental LIS values. We chose a comparable arrangement for all n possibilities to obtain compatible positional parameters for Eu^{3+} in all ($n/2$) complexes ($n/2$ complexes are characterized by n principal magnetic axes, 2 axes per complex). This allows to calculate the magnetic field strength for *all* possible complex geometries using only *one* (variable) Eu^{3+} position but an *n -fold set* of (fixed) proton positions. This means that the relative Eu^{3+} position within the framework of the three coordinating oxygen atoms is the same for all possible complexes (same bond length, same out-of-aromatic-plane angle and equidistant from the two oxygens in the bidentate complexes).

The model: *one substrate geometry* and *n magnetic axes* was therefore changed to the computationally simpler alternative but equivalent model: *one magnetic axis* but *n coordinate sets* for the protons which are merged to *one n -fold set of proton positions* (compare Refs. [16, 20]).

Now the contributions of the magnetic field strengths (geometrical factors [17, 18]) for the n -fold set of coordinates (always n corresponding positions for each proton) are calculated by means of the McConnell-Robertson equation [17, 18]. Then the calculated geometrical factors for corresponding proton positions are averaged to a mean value of all n contributions. The values for all protons are finally scaled to the experimental values, the quality of the fit being characterized as usual by the R -factor [17, 18].

Then the next Eu^{3+} position (within the O–O symmetry plane) is checked in the same manner: Eu^{3+} is moved, all coordinates of the protons remain constant. The position with the R -factor minimum is considered to be the best possible fit for the complex geometry of a particular substrate conformation. Different populations for the n sets of proton coordinates may be introduced in the averaging procedure; however, we found always equipopulation of all Eu^{3+} positions within the 1,2,3-trimethoxy group (a different population may be only expected if some severe sterical hindrance in the vicinity of the coordination sites is present).

These reasonable assumptions, namely identical coordination geometries for all possible bidentate complexes and restriction of the lanthanide ion position to the plane bisecting the two coordinating atoms of the bidentate complexes (symmetrical Eu^{3+} position equidistant from both oxygen atoms), reduces the variable Eu^{3+} positional parameters in the complete calculation to only two: (i) the distance $\text{O} \cdots \text{Eu}^{3+}$ and (ii) an angle defining the deviation of the Eu^{3+} position from the aromatic plane.

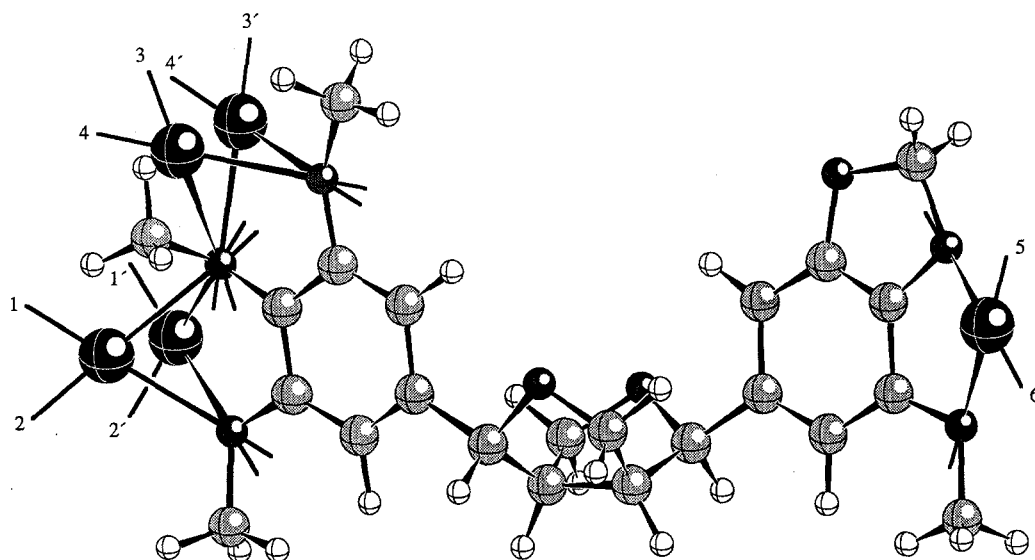


Fig. 1. Possible principal magnetic axes for Eu(III) complexes of compound 2

If the lanthanide ion is not found within the plane defined by the aromatic system, an additional complication arises; in this case there are two equally possible positions on both sides of the benzene ring which have to be considered in the calculation (the program allows also different populations for these symmetric positions, however, in all cases an equal population on both sides of the aromatic plane gave the best fit).

Figure 1 shows all possible principal magnetic axes for the rather complicated case of diasartemin (2). Axes 1–4 for the 1,2,3-trimethoxy coordination (1'–4' for the symmetric positions on the other side of the benzene plane). These axes are for instance sufficient for compound 1. In the sesartemins 2 and 3, however, there

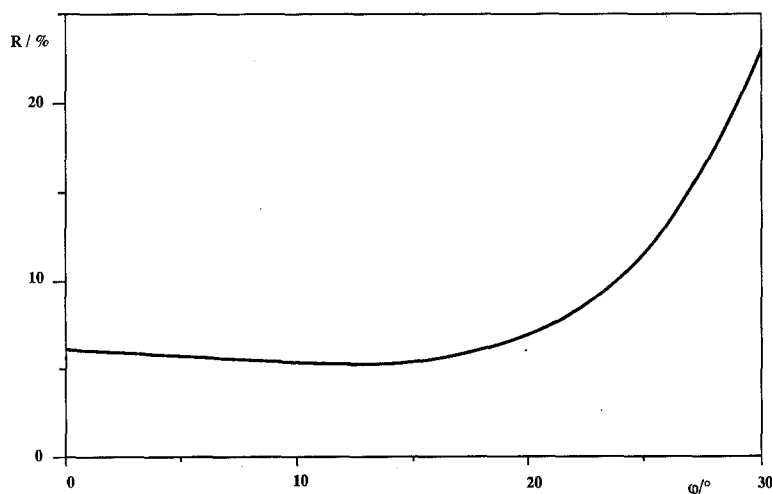
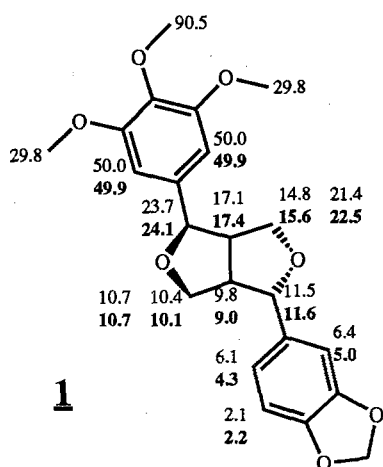
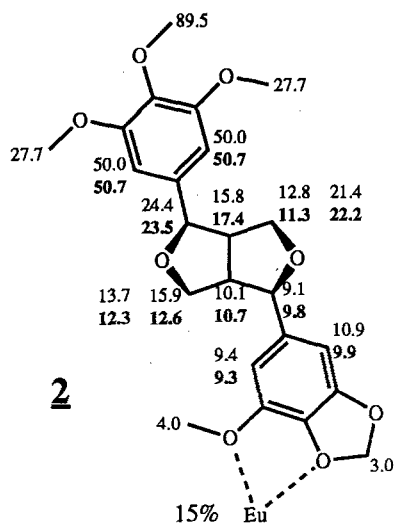


Fig. 2. Change in the quality of the fit (*R*-factor) in dependence of the Eu(III) deviation from the aromatic plane (angle between the planes Eu/O/O and phenyl/O/O)



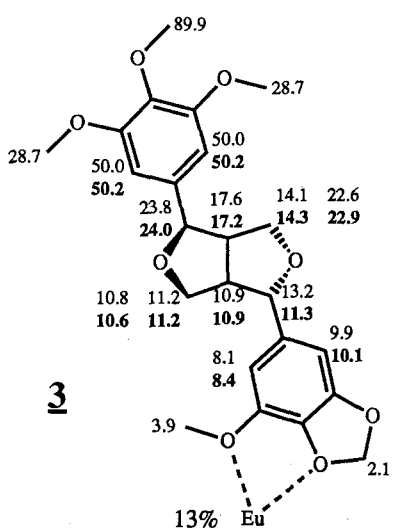
Epiashantin : $d = 2.3 \text{ \AA}$, $\phi = 13^\circ$

$$\begin{pmatrix} \text{ax-eq} \\ \text{syn-anti} \\ \text{boat-chair} \end{pmatrix} \begin{matrix} \Psi_1 = 100^\circ \\ \Psi_2 = 125^\circ (R = 5.42\%) \\ \Psi_2 = 295^\circ (R = 5.51\%) \end{matrix}$$



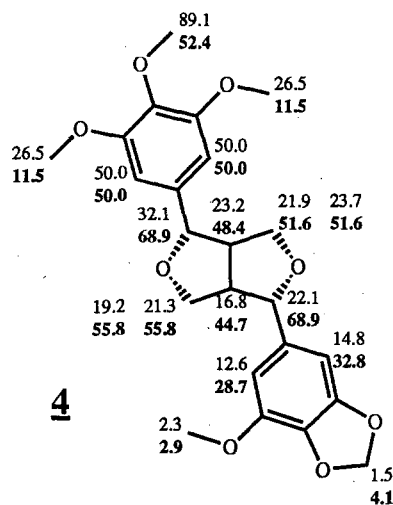
Diasesartemin : $d = 2.4 \text{ \AA}$, $\phi = 24^\circ$

$$\begin{pmatrix} \text{ax-ax} \\ \text{syn-syn} \\ \text{boat-boat} \end{pmatrix} \begin{matrix} \Psi_1 = 120^\circ \\ \Psi_2 = 115^\circ (R = 4.82\%) \\ \Psi_2 = 290^\circ (R = 6.78\%) \end{matrix}$$



Episesartemin B : $d = 2.5 \text{ \AA}$, $\phi = 27^\circ$

$$\begin{pmatrix} \text{ax-eq} \\ \text{syn-anti} \\ \text{boat-chair} \end{pmatrix} \begin{matrix} \Psi_1 = 90^\circ \\ \Psi_2 = 130^\circ (R = 2.93\%) \\ \Psi_2 = 280^\circ (R = 2.99\%) \end{matrix}$$



Sesartemin : experimental values
with $\text{Eu}(\text{fod})_3$ and $\text{Eu}(\text{dpm})_3$

$$\begin{pmatrix} \text{eq-eq} \\ \text{anti-anti} \\ \text{chair-chair} \end{pmatrix}$$

Fig. 3. Experimental $[\text{Eu}(\text{fod})_3]$ and calculated LIS values. Note: for 1–3 the bold numbers represent the calculated values, for 4 the bold numbers give additional experimental values with $\text{Eu}(\text{dpm})_3$ as shift reagent; normal printed numbers indicate always experimental values for the $\text{Eu}(\text{fod})_3$ complexes of 1–4. For better comparison the experimental data are normalized to a LIS-value of 50.0 for the aromatic protons next to the trimethoxy group since these protons are comparable for all compounds 1–4; one tenth of the listed values corresponds to the so-called 1:1 complex, typical values for the central OMe group of the trimethoxy moiety are 9 ± 1 ppm [9] (ca. 90 in the presentation above)

is still a further complication due to some minor complexation at a methoxy-methyleneoxy bidentate coordination site on the other aromatic ring; axes 5 and 6 take care for this additional contribution to the LIS values (about 15% population relative to the total complexation improved the fit considerably, vide infra).

The procedure outlined above may appear rather complex and artificial, however, the basic idea is strikingly simple: The complexing behaviour is reduced to symmetrical and topologically equal bidentate complexes. The fit allows actual not very much freedom in the choice of the lanthanide ion position since the variation of the $\text{O} \cdots \text{Eu}^{3+}$ bond length and the movement of the lanthanide ion position out of the aromatic plane is rather limited due to stereochemical reasons: the bidentate complexing itself determines already to a large extent the lanthanide ion position. Fig. 2 shows the dependence of the *R*-factor from the out of plane movement of the lanthanide ion; within reasonable limits (0° – 20°) the *R* factor does not change very much (5.4–6.3% for compound **1**, s. Fig. 2). The dependence of *R* from the ion distance is also not dramatic within the reasonable limits of 2.2–2.7 Å (e.g. for **1** as a typical example: $R_{\min} = 5.4\%$ at 2.3 Å, $R = 6.1\%$ at 2.6 Å). As a consequence it is possible to predict a reasonably accurate lanthanide ion position in case there are not enough reliable LIS values for an extensive fitting procedure. The knowledge about the most probable coordination geometry was for instance utilized for the estimation of the LIS contribution due to the less populated methoxy-methylenedioxy bidentate coordination site in compounds **2** and **3** (axes 5 and 6 in Fig. 1).

Figure 3 shows all experimental $[\text{Eu}(\text{fod})_3]$ and calculated LIS values for compounds **1**–**3** and the experimental LIS data with $\text{Eu}(\text{fod})_3$ and $\text{Eu}(\text{dpm})_3$ as reagents for compound **4**.

Epiashantin (**1**)

For compound **1** the experimental LIS values are solely due to coordination at the trimethoxy group. This is indicated by the strong linearity of all LIS values in dependence from the reagent concentration [no deviation up to a reagent : substrate ratio ($R_0 : S_0$) of 0.5 : 1]. Therefore, this molecule should offer a good possibility to test the usefulness of our LIS-simulation model for trimethoxy coordination. Since the geometry of the two fused five-rings of the tetrahydrofurofuran system should be rather rigid, it was taken from the X-ray structure of **3**, which belongs to the same type (“epi”-series with “ax, eq” substituents, giving “endo–exo” or “boat–chair” conformation of the furofuran system [11], compare Fig. 3).

One may distinguish three types of tetrahydrofurofuran geometries for this type of compounds, depending on the stereochemistry of the substitution at positions 1 and 4 [11]: (i) The “endo–endo type” (endo positions for both oxygen atoms relative to the second fused five-ring); one may also use the term “boat–boat type” to characterize the conformation of the overall 8-ring (compare compound **2** of Fig. 3, note that the bridge hydrogens at positions 3 a and 6 a are below C 3 a and C 6 a, the four carbon atoms C 1, C 3, C 4, and C 6 are above C 3 a/C 6 a and the two oxygens O 2 and O 5 again above C 1, C 3, C 4, C 6, resulting in an overall boat–boat shape of the system [this corresponds to the substitution type formerly called axial-axial [11] and is typical for the di-tetrahydrofurofuran lignan series, e.g. diasesartemin (**2**)]. (ii) the “endo–exo” or “boat–chair” type for the epi-lignan series [e.g. epiashantin (**1**) or episesartemin (**3**) where one oxygen is endo to the second ring (partial boat structure), the second one exo (down in the presentation used in Fig. 3,

partial chair structure)], corresponding to the ax-eq type of substitution in the previously used (actually wrong [11]) classification. (iii) The “exo-exo” or “chair-chair” type (in the formerly used classification the C1, C4 “eq-eq” substituted compounds of the tetrahydrofurofuran type, e.g. compound 4).

In contrast to the 1,4-substituted fused five-ring skeleton with a clearly favoured (“rigid”) conformation (which was also shown in relevant MM2 calculations) the rotation of the aromatic substituents about the C1 (or C4)-C1 (aryl) bonds remains an open question. Therefore, the aromatic substituents were moved in increments about the corresponding bonds and the best possible fit was determined following the procedure outlined in the paragraphs above.

Two angles Ψ_1 and Ψ_2 have been defined: Ψ_1 is the torsional angle C1a-C1-C1(aryl)-C6(aryl) for the trimethoxyphenyl substituent, Ψ_2 is defined in the same manner for the other phenyl substituent. For **1** the best possible fit was found for torsional angles of $\Psi_1 = 100^\circ$ and either $\Psi_2 = 125^\circ$ (with an *R* factor of 5.42%) or $\Psi_2 = 295^\circ$ (with an *R*-factor of 5.51%) (Fig. 3). For Ψ_1 the answer is clear cut, because due to the symmetry of the trimethoxyphenyl substituent the conformations with Ψ_1 and $\Psi_1 + 180^\circ$ are equivalent. In the case of Ψ_2 the two conformers with 125° and 295° (which is equal to $125 + 170^\circ$) give a comparably good fit and no decision based on the LIS data is possible (compare also the related epi-compound **3**).

However, it is important to note that both possibilities ($\Psi_2 = 125^\circ$ and 295°) correspond to roughly orthogonal conformations of the phenyl ring relative to the five-ring system where it is attached. This seems to be a general result which was observed more or less uniformly for all aryl substituents of all tetrahydrofurofuran lignans where a conformational analysis was carried out.

Diasartemin (2)

In the case of compound **2** a non-linearity in the lanthanide induced shifts with increasing reagent concentration was observed. The protons of the trimethoxyphenyl rest and some proton signals of the closer 5-ring were still linear at $L_0:S_0 = 0.5:1$, but especially the protons of the second aryl substituent and some tetrahydrofurofuran proton resonances close to the methoxy-methylenedioxyphenyl rest showed a clear deviation, the signals “moving too fast” with increasing reagent concentration. This points clearly towards some coordination at the second aryl moiety competing with the still dominant trimethoxy coordination. To account for this we used a somewhat modified procedure for the quantitative LIS simulation. In the first step of the calculation the Eu^{3+} positions at the trimethoxy rest and the torsional angle Ψ_1 were determined without using the protons exhibiting pronounced non-linearity of LIS values (if all LIS were used, the calculated values for “non-linear” protons far from the trimethoxy group, especially for the second phenyl rest, were too low and no *R*-factor below 10% could be obtained*). In a

* For molecules of medium size (ca. 10 independent LIS values) *R* factors above 10% indicate some wrong conditions in the calculation, either wrong model assumptions for the complexation or an incorrect substrate geometry. *R* factors in the range of 5% or below may be considered to represent a good fit, *R* below 8% is still reasonable

second step all LIS were used, but a further bidentate coordination was introduced at methoxy-methylenedioxy (compare Fig. 1). This lanthanide ion position was presumed to be within the aromatic plane and an $\text{O} \cdots \text{Eu}$ distance of 2.5 \AA was taken [since this minor coordination adds only a small contribution to the final LIS values, the assumption of a typical (average) lanthanide ion position is justified; compare the previous section Computational Model]. The only additional variable parameter for the improvement of the fit was therefore the relative population of this additional complexation. The best fit, with an R factor of 4.82%, was obtained for $\Psi_2 = 115^\circ$ and 15% Eu^{3+} complexation at methoxy-methylenedioxy (Fig. 3).

A second, somewhat less good solution ($R = 6.78\%$) was characterized by $\Psi_2 = 290^\circ$ ($115 + 175^\circ$). Again the conformer with essentially equal torsion of the basic phenyl residue but symmetrically changed aromatic substituents gives a clear R factor minimum. However, in this case the R -factor difference of both suggested conformations is significantly larger than for compound 1 (and 3, see below).

The conformer with $\Psi_2 = 115^\circ$ ($R = 4.82\%$) seems to be the dominant one in solution. Interestingly enough the same conformation was obtained in the X-ray structure of compound 2 (compare Fig. 4 of this paper with Fig. 1 a of Ref. [11], showing the molecule from a comparable view). In the conformer with $\Psi_2 = 290^\circ$ the methoxy group of the methoxy-methylenedioxy phenyl rest would adopt a position above the tetrahydrofurofuran system, pointing towards the trimethoxyphenyl moiety, which might have some unfavourable effects.

Supporting Force Field Calculations

In order to obtain some information on the energetic relations of these possible conformers we performed force field calculations (MM2) on compounds 2–4, which are representatives for the above mentioned types of diaryltetrahydrofurofuran lignans (boat–boat, boat–chair, and chair–chair). It turned out that the ground state geometries were very similar to the ones obtained experimentally by the LIS technique. In all cases two favoured conformations were found for the methoxy-methylenedioxyphenyl rest, the energy difference of both was within the error of the calculation. The energy profile of the rotation Ψ_2 (as well as Ψ_1) was very flat

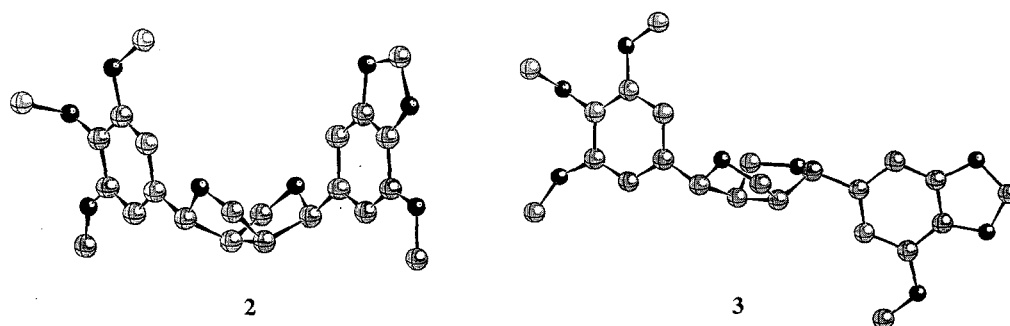


Fig. 4. Ball & Stick presentation of the solution geometries for compounds 2 and 3; the structures may be directly compared with the X-ray structures (Ref. [11], Fig. 1). for 3 only one of the two possible conformers is shown ($R = 2.93\%$), the X-ray conformer with $-\text{OMe}$ up and $-\text{OCH}_2\text{O}-$ down [11] gives also a very good LIS fit ($R = 2.99\%$, compare Fig. 3)

and the results – energy value and angle – depended to some degree on the starting geometry. However, approaching the energy minimum from both sides and using different starting geometries allowed to obtain reliable MM2-values for Ψ_1 and Ψ_2 with an accuracy of at least $\pm 10^\circ$. On the other hand, the energy values for the two corresponding conformers for all calculated compounds **2–4** were too close ($\pm 0.3 \text{ kcal mol}^{-1}$, with overlapping scattering for both conformers) and *no decision* in favour of one or the other conformer with respect to the torsion Ψ_2 was possible by MM2 calculations.

The same problem, two equal good solutions (Ψ_2 or $\Psi'_2 = \Psi_2 + 180^\circ$) was encountered in the LIS analysis of compound **1** and **3** as well. However, it should be pointed out that the very often quite similar behaviour of energy profiles and *R*-factors allows by no means any kind of direct conclusions [21]. More or less similar energy values for two conformers mean comparable probability for both to represent the true geometry of the substrate in equilibrium (including quantitative evaluation in terms of relative populations of conformers). More or less equal LIS values mean two possible geometries for a substrate, either *one* or the *other* or *any mixture of both* could be the truth. If the important pilot protons for a rotation move along “isomagnetic” lines (insensitive to changes due to the structure of the magnetic field) the *R* factors are insensitive to conformational changes as well and no decision is possible. In other words, equal *R* factors for different conformations can happen accidentally as well. If this is the case, one has to accept that no clear cut decision is possible from the LIS data. This was the case for compounds **1** and **3** concerning the torsional angle of the second phenyl rest (Ψ_2 and/or $\Psi'_2 = \Psi_2 + \text{ca. } 180^\circ$). For these two molecules both methods, LIS and MM2 calculations were not able to discriminate the two conformers.

However, for compound **2** we have the fortunate case that one of the two possible MM2 conformers is characterized by a significantly better *R* factor in the LIS simulation. The corresponding torsional angles for the LIS, MM2, and X-ray results are compiled in Table 1. For compound **2** the data are rather consistent for all three methods of conformational analysis. This is very much in favour of the usefulness of the outlined trimethoxy coordination model for LIS simulation. In the case of compound **2** the LIS method allowed a decision while the MM2 cal-

Table 1. LIS, MM2 and X-ray results for the torsional angles Ψ_1 and Ψ_2 characterizing the torsion of the aromatic planes relative to the tetrahydrofuran skeleton (Ψ_1 for the trimethoxyphenyl rests, Ψ_2 for the other aromatic substituent); if two angles are given, the particular method does not discriminate between the two conformers

Compd.	Torsion	LIS	MM2	X-ray [11]
2	Ψ_1	120°	119°	109°
	Ψ_2	115°	104°/284°	94°
3	Ψ_1	90°	110°	127°
	Ψ_2	130°/280°	116°/296°	293°
4	Ψ_1	—	95°	—
	Ψ_2	—	110°/290°	—

culations did not. We consider both methods as complementary tools, which should be used in combination for sophisticated problems of conformational analysis.

Using the dihedral driver of the MM2 program, we have also estimated the barriers of rotation about Ψ_1 and Ψ_2 . The barriers depend on the configuration of the phenyl rest (which is always pseudoequatorial) relative to the neighbouring oxygen: phenyl rests attached to an exo-oxygen five-ring (partial chair conformation) have rotational barriers of ca. 10 kcal mol^{-1} , phenyl rests attached to an endo-oxygen five-ring (partial boat conformation) have rotational barriers which are at least twice as high. In both cases, but especially pronounced for the latter type, the tetrahydrofurofuran system suffers some distortions when the bulky substituents of the phenyl ring pass by during rotation.

Episesartemin B (3)

The LIS simulation of compound **3** followed the procedure described for **2**: again non-linearity for LIS of protons close to the methoxy-methylenedioxyphenyl rest; therefore calculation in two separate steps, fit 1 for the partial structure close to the trimethoxyphenyl moiety ($\Psi_1 = 90^\circ$), final fit 2 assuming a further bidentate complexation site at the second aromatic rest (13% compared to 87% around the trimethoxy sites, s. Fig. 3).

The final result is similar to the one of the related compound **1** (also boat – chair type): equal good R factors for two possible solutions for Ψ_2 (either 130° or 280° with R factors of 2.93 or 2.99%, respectively); see Fig. 4. The general result concerning this torsion Ψ_2 is that the aromatic plane is about perpendicular to the attached five-ring. The MM2 results are consistent with the LIS geometries (also two comparable minimum geometries, s. Table 1), the X-ray data gave only one conformer in the crystalline state ($\Psi_2 = 293^\circ$), which corresponds to the LIS conformer with $\Psi_2 = 280^\circ$.

Sesartemin (4)

The LIS data of compound **4** differ completely from compounds **1–3** (compare the values given in Fig. 3). The data obtained with $\text{Eu}(\text{fod})_3$ as shift reagent showed much too high values for the protons close to the methoxy-methylenedioxyphenyl rest. However, even the simulation including the corresponding bidentate coordination (which was very successful for **2** and **3**) did not give any fit with an R factor below 20%. So we tried $\text{Eu}(\text{dpm})_3$, because this shift reagent is usually less aggressive in its coordinating behaviour and a more selective coordination should take place. However, the behaviour of substrate **4** towards $\text{Eu}(\text{fod})_3$ was rather unexpected: (i) the lines became very broad even at low reagent concentrations, which usually indicates an uncontrolled poly-coordination with a variety of important complex geometries in solution, and (ii) the LIS values of the tetrahydrofurofuran protons were increased considerably in comparison with the $\text{Eu}(\text{fod})_3$ values; a closer inspection of the $\text{Eu}(\text{dpm})_3$ data [compare Fig. 3, bold values for **4** ··· $\text{Eu}(\text{dpm})_3$] shows that the values of the tetrahydrofurofuran protons are roughly symmetrical with respect to the symmetry of this fused ring system itself. Both observations, (i) and (ii), imply that some strong, unexpected and unusual complexation must have been occurred involving the two oxygen atoms of the symmetrical tetrahydrofurofuran moiety (the deviations from a complete symmetry of the LIS data is easily explained by the still important complexation at the trimethoxyaryl unit, compare the LIS values in Fig. 3).

The question arises, which type of complexation this could possibly be. The most reasonable explanation is the assumption of a bidentate complex involving a dimeric reagent molecule. It is well known that the shift reagents have a tendency towards dimerization and the formation of substrate-dimer reagent complexes is always possible [22]; however, in the coordination to usual substrates this reagent dimers are of less importance.

In the case of the chair – chair conformation adopted by the tetrahydrofurofuran system in compound **4** the lone pairs of the two oxygen atoms seem to be ideally orientated for this type of complexation. As can be seen from the MM2 calculations, the distance of the two oxygen atoms is ca. 4.3 Å and the lone pair distance (compare Fig. 5) is 4.6 Å. This is prohibitive for a bidentate complex with a monomeric reagent molecule (distances too large). The geometry, however, seems to be ideal for a dimeric reagent. Based on the data of a praseodyme-dimer (Pr···O···Pr distance 4.1 Å [23]), the Eu – Eu distance in an analogous Eu···O···Eu dimer is expected to amount to ca. 4.5 Å (typical Eu···Eu bond 3.99 Å, Pr···Pr bond 3.64 Å [24]). Usually five-membered ethers are very inefficient complexation sites for shift reagents and the very significant increase of the complexation constant for the cyclic ether oxygens in **4** is only explainable assuming a bidentate complex of the type shown schematically in Fig. 5 and/or some closely related species [22].

However, the quantitative LIS simulation of compound **4** was not possible and since no X-ray data are available either, only the MM2 computed geometry is given in Table 1. The partial geometries of both exo – exo (chair – chair) rings, including the aromatic substituents, were found to be absolutely comparable with the exo five-ring partial structure of the endo – exo compound **3**.

Calculation of the CD Couplet for the Aromatic 1B_g Band of Compounds **2** and **4**

The detailed knowledge on the solution geometry of tetrahydrofurofuran lignans should provide a rather reliable basis for a quantitative prediction of the CD bands based on the coupled oscillator model. Previous attempts include a correct qualitative evaluation for the sign of the couplet [11] for **2** and a quantitative estimation for **2** and **4** [10] using wrong assumptions concerning the geometry (*and* the position of the A and B band).

With respect to the aromatic chromophores, sesartemin (**4**, boat – boat type) and diasartemin (**2**, chair – chair type) possess practically C_2 symmetry. Since the

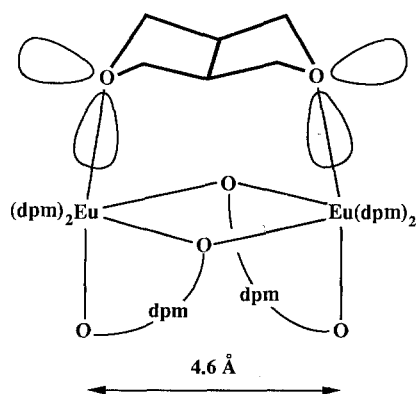


Fig. 5. Schematic presentation of the bidentate complex of compound **4** with a dimeric Eu (III) reagent species

chromophors are not connected by conjugation but nevertheless rather close to each other, all conditions for a calculation of the CD bands due to the coupled oscillator model are fulfilled [25]. The aromatic short wave band (1B_b transition at ca. 207 nm for the trialkoxyphenyl system) has a strong electric transition moment and the coupling intensity is rather high for **2** but surprisingly low for **4**. For all boat–boat type (former ax-ax type, e.g. **2**) of tetrahydrofurofurans the coupling effects are rather strong with a $\Delta(\Delta\epsilon)$ of $> 100!$ [10]. The effects are much smaller for the chair–chair type [10]; for **4** $\Delta(\Delta\epsilon) < 10$ (s. Exp.). Since the distance d between the two coupling systems is in the same order of magnitude for both types and d represents a *linear* factor in the corresponding equation for R^A (or $-R^B$) the drastic difference must be due to a different orientation of the transition moments (and the chromophors) in space, which is reflected in the positional angles α , β , and γ . The larger value for d in **4** should actually *increase* the rotator strength relative to **2**, the very low coupling effect with a drastic *decrease* of the rotator strength for **4** must therefore be due to either β or γ being close to 90° (cosinus close to zero, compare formula in Table 2).

Within the stereochemically determined boat/boat and chair/chair series the data are very similar [10]. The CD calculations (or “quantitative estimations”) are therefore valid for the entire series of related tetrahydrofurofuran lignans.

Table 2 lists all data and formula used in the computations. Following successive steps are necessary:

(i) *Extraction of experimental UV and CD parameters from the measured spectra.* The UV data give (via oscillator strength) the value for the electrical transition moment which in turn is needed for further calculations (the oscillator strength turns out to be ~ 1 , which is characteristic for fully allowed transitions). Evaluation of the CD curves give experimental values for band splitting and rotator strength of the couplet for the 1B_b band.

(ii) *Calculation of the characteristic parameters for the circular dichroism of the 1B_b couplet.* The two relevant formula for band splitting and rotator strength need (apart from the wave number and the electrical transition moment of the corresponding UV transition, and the constants h , c , and π) some geometrical parameters concerning the topology of the electronic transition. For the latter, one needs to know the relative position of the two coupling transitions within the molecule, which may be derived from the knowledge of the direction of the transition in the isoalted chromophor (estimated by PPP calculations [10]), and knowledge of the solution geometry of the molecule. Then the distance d of the chromophors (distance of the centers of the aromatic ring) and the directional parameters α , β , γ within the local coordinate systems [25] may be obtained.

The calculated parameters for the CD couplets of **2** and **4** agree in general with the experimental data. The band splittings are reproduced excellently, the rotator strengths are somewhat problematic. The calculated rotator strengths are very sensitive to relatively small changes in the angles α , β , γ : in the case of compound **2** (large effect) the calculated order of magnitude and the sign with a negative A-band at lower wave length and a positive B-band at larger wavelength is correct; the absolute value is somewhat overestimated which may be due to some error in the angles α , β , γ (a decrease of 10° for the angle β or γ gives already a rotator strength of $3 \cdot 10^{-38}$, which is very close to the experimental value). However, the uncertainty in the relative angles of the transition moment becomes the crucial

Table 2. Experimental and calculated data (including formulas and Refs.) for the calculation of the short wave length couplet in the CD of compounds **2** and **4**

	2	4	Formula used	[Ref.]
Experimental data				
UV (equal for 2 and 4)				
$\bar{\nu}_{\max}$, ϵ_{\max}	$4.8 \cdot 10^4 \text{ cm}^{-1}$, 80 000 l mol ⁻¹ cm ⁻¹			
$\Delta\bar{\nu}_{0.5}$	$2.8 \cdot 10^3 \text{ cm}^{-1}$			
f	~ 1		$f = 4.34 \cdot 10^{-9} \epsilon_{\max} \Delta\bar{\nu}_{0.5}$	[26]
μ	$6.6 \cdot 10^{-18} \text{ [cgs]}$		$\mu = 1.46 \cdot 10^3 \sqrt{f/\bar{\nu}_{\max}} \text{ [Debye]}$	[27]
CD				
$\bar{\nu}_0$	$4.78 \cdot 10^4 \text{ cm}^{-1}$	$4.78 \cdot 10^4 \text{ cm}^{-1}$		
$\Delta\bar{\nu}_{\text{exp}}$ [10] ^a	1800 cm^{-1}	1000 cm^{-1}		
R_{exp} [10] ^a	$2.5 \cdot 10^{-38} \text{ [cgs]}$	$0.2 \cdot 10^{-38} \text{ [cgs]}$	$R = \frac{0.204 \cdot 10^{-38} \Delta\epsilon_{\max} \Delta\nu_{0.368}}{\bar{\nu}_{\max}}$	[27]
Calculations				
α, β, γ ^b	$148^\circ, 111^\circ, 68^\circ$	$158^\circ, 95^\circ, 114^\circ$		
d ^b	$7.23 \cdot 10^{-8} \text{ cm}$	$8.67 \cdot 10^{-8} \text{ cm}$		
$\bar{\nu}_A - \bar{\nu}_B = \Delta\bar{\nu}_{\text{per}}$	1700 cm^{-1}	1280 cm^{-1}	$\bar{\nu}_A - \bar{\nu}_B = \frac{2 \mu^2}{h c d^3} (\cos^2 \gamma - \cos^2 \beta + 2 \cos^2 \alpha)$	[25]
R^B ^c	$6.4 \cdot 10^{-38} \text{ [cgs]}$	d	$R^A = -R^B = \pi \bar{\nu}_0 d \mu^2 \cos \beta \cos \gamma$	[25]

^v frequency [s⁻¹], $\bar{\nu}$ wave number [cm⁻¹], ϵ molar extinction coefficient, f oscillator strength, μ electrical transition moment, $\Delta\bar{\nu}_{0.5}$ $\bar{\nu}$ band width at half height, $\bar{\nu}_0$ wave number of the center between the A and B band, $\Delta\bar{\nu}_{\text{exp}}$ experimental band splitting of the couplet [cm⁻¹], R rotator strength, $\Delta\epsilon$ circular dichroism [l mol⁻¹ cm⁻¹], $\Delta\nu_{0.368}$ band width at 0.368 of the total height, $h = 6.626 \cdot 10^{-27}$ erg s, $c = 3 \cdot 10^{10}$ cm s⁻¹

^a Result of a Gauß-curve analysis of the experimental CD [10]

^b The direction of the transition moment was derived from PPP-calculations [10]; the geometries of **2** and **4** giving the final numerical values for the distance d between the two coupling chromophores and the directional angles α, β, γ were taken from MM2 calculations

^c The band at longer wavelength (smaller ν) determining the sign of the couplet for **2** is the positive B-band

^d As β is only slightly different from 90° a safe prediction of the absolute value and the sign of R is not possible

point for compound **4** (compare Table 2). In this case a decrease of 10° for γ would not cause much trouble for the band splitting (\cos^2 in the formula), but would be fatal for the rotator strength which would change its sign, going through $R=0$ at 90° ; exactly this happened in the calculation of R for compound **4**. However, it should be mentioned that the prediction of rotator strengths (and signs) for weak coupling effects is generally problematic, because small deviations in the topology of a system have large effects on the calculation. Some corrections in the geometry (for instance in the torsional angles) *and/or* a slight displacement of the direction of the transition moment would allow to find some proper correction; however, the result would be speculative.

So we confine ourselves to the following result: the agreement between experimental and theoretical values of the band splittings (which are less sensitive to unavoidable errors in the localization of the electric transitions) is excellent; the experimental rotator strengths are less well reproduced but they agree within a maximum error of $\sim 10^\circ$ for the positional angles. The large effect for **2** is described correctly (in this case the sign of the couplet-bands can be safely calculated), for **4** a small effect is theoretically predicted and experimentally found (due to γ being close to 90°). The trend of large CD coupling effects for boat–boat type lignans and small amplitudes for the 1B_b couplet of the chair–chair type is perfectly consistent with the found solution geometries.

Acknowledgements

We wish to thank Prof. Dr. H. Greger, Institute of Botany, University of Vienna, for sample of lignans. Further we thank Dr. W. Weissensteiner for his valuable and skillful help in the course of the MM2 calculations and Mag. H. P. Kählig for NMR spectra. Support by the “Österreichischer Fonds der wissenschaftlichen Forschung” (proj. no. 5840) and by the “Hochschuljubiläumsstiftung der Stadt Wien” is gratefully acknowledged.

Experimental

The compounds have been isolated from *Artemisia absinthium* L. [9] by column chromatography and MPLC, the purity was checked by $^1\text{H-NMR}$ and HPLC. The-NMR spectra (δ/ppm) were recorded on a Bruker WM 250 instrument, for CD and UV spectra the instruments Jobin Yvon dichrograph MARK III and Perkin-Elmer Lambda 5 were used. The force field calculations were performed using the program MM2(87) [28, 29].

The characteristic data of compounds **1–4** were already given in [9, 10]. However, in the following we list some supplementary data (CD for **4**) and a more detailed assignment of the $^1\text{H-NMR}$ resonances of **1–4** based on the better resolution of the instrument and the LIS analysis.

Epiashantin (**1**): $^1\text{H-NMR}$ (CDCl_3 , δ/ppm): 6.87 (d, 1 H, $J=1.8$ Hz, 2''-H), 6.83 (dd, 1 H, $J=1.8$ and 8.0 Hz, 6''-H), 6.78 (d, 1 H, $J=8.0$ Hz, 5''-H), 6.58 (s, 2 H, 2'-H, 6'-H), 5.96 (s, 2 H, 8''-H), 4.85 (d, 1 H, $J=6.0$ Hz, 1-H), 4.43 (d, 1 H, $J=7.0$ Hz, 4-H), 4.12 (d, 1 H, $J_{3\text{eq}}=9.6$ Hz, 3 ax-H), 3.88 (s, 6 H, 8'-H, 12'-H), 3.86 (s, 3 H, 10'-H), ~ 3.86 (dd, 1 H, 3 eq-H), ~ 3.86 (dd, 1 H, 6 eq-H), 3.37 (ps. quin, 1 H, $J_{1, 3a, 6ax, 6eq} \sim 8.0$ Hz, 6a-H), 3.33 (ps. t, 1 H, $J_{6\text{eq}, 6a} = 8.0$ Hz, 6 ax-H), 2.88 (ps. q, 1 H, $J_{4, 6a, 3\text{eq}} \sim 7.0$ Hz, 3 a-H).

Diasartemin (**2**): $^1\text{H-NMR}$ (CDCl_3 , δ/ppm): 6.58 (s, 2 H, 2'-H, 6'-H), 6.56 (s, 1 H, 2''-H), 6.54 (s, 1 H, 6''-H), 5.97 (s, 2 H, 8''-H), 4.92 (d, 1 H, 4-H), 4.89 (d, 1 H, 1-H), 3.90 (s, 3 H, 11''-H), 3.88 (s, 6 H, 8'-H, 12'-H), 3.86 (s, 3 H, 10'-H), 3.73 (d, 1 H, $J_{6\text{eq}} \sim 6.0$ Hz, 6 ax-H), 3.71 (d, 1 H, $J_{3\text{eq}} \sim 6.0$ Hz, 3 ax-H), 3.55 (m, 2 H, 3 eq-H, 6 eq-H), 3.18 (m, 2 H, 3 a-H, 6 a-H).

Episesartemin (**3**): $^1\text{H-NMR}$ (CDCl_3 , δ/ppm): 6.56 (s, 2 H, 2'-H, 6'-H), 6.54 (s, 2 H, 2''-H, 6''-H), 5.96 (s, 2 H, 8''-H), 4.84 (d, 1 H, $J=5.2\text{ Hz}$, 1-H), 4.39 (d, 1 H, $J=7.6\text{ Hz}$, 4-H), 4.12 (d, 1 H, $J_{3\text{eq}}=9.2\text{ Hz}$, 3 ax-H), 3.89 (s, 3 H, 11''-H), 3.87 (s, 6 H, 8'-H, 12'-H), ~ 3.87 (dd, 1 H, 6 eq-H), 3.85 (s, 3 H, 10'-H), ~ 3.84 (dd, 1 H, 3 eq-H), 3.31 (m, 2 H, 6 ax-H, 6 a-H), 2.87 (ps. q, 1 H, $J_{3\text{eq},4,6a}\sim 7.0\text{ Hz}$, 3 a-H).

Sesartemin (**4**): $^1\text{H-NMR}$ (CDCl_3 , δ/ppm): 6.54 (s, 2 H, 2'-H, 6'-H), 6.52 (s, 1 H, 2''-H), 6.51 (s, 1 H, 6''-H), 5.94 (s, 2 H, 8-H), 4.70 (d, 2 H, 1-H, 4-H), 4.22–4.30 (m, 4 H, 3 ax-H, 3 eq-H, 6 ax-H, 6 eq-H), 3.89 (s, 3 H, 11''-H), 3.85 (s, 6 H, 8'-H, 12'-H), 3.81 (s, 3 H, 10'-H), 3.06 (m, 2 H, 3 a-H, 6 a-H). CD [*EtOH* at $c=0.25\text{ mmol/dm}^3$, λ/nm ($\Delta\epsilon/\text{l mol}^{-1}\text{ cm}^{-1}$): 277 (max., +0.72), 285 (min., +0.2), ca. 237 (center of a steady broad increase, +1.2), 216 (max., +7.3), 208 (± 0.0), 200 (sh. or min., ca. -1.8); corresponding UV [*EtOH*, λ/nm ($\Delta\epsilon$): 274.5 (2300), 235 (sh., 12600), 208.5 (80000).

Lanthanide Induced Shifts

Increasing amounts of $\text{Eu}(\text{fod})_3$ [in one case (**4**) also $\text{Eu}(\text{dpm})_3$] were added to solutions of ca. 5 mg lignan in 0.5 ml of CDCl_3 . The LIS for the concentration ratio $R_0:S_0=1:1$ ("1:1 complex") were obtained by extrapolation of 3–5 different reagent concentrations in the range of $R_0:S_0=0.0\text{--}0.7:1$. The calculations of simulated LIS were performed on an Apple Macintosh PC using a special program ("LIS3ME"). For features of this program compare the section Results and Discussion, a flow diagram is given in [30]. The results are summarized in Fig. 3.

References

- [1] Birch A. J., Macdonald P. L., Pelter A. (1967) *J. Chem. Soc. (C)*: 1968
- [2] Atal C. K., Dhar K. L., Pelter A. (1967) *J. Chem. Soc. (C)*: 2228
- [3] Briggs L. H., Cambie R. C., Couch R. A. F. (1968) *J. Chem. Soc. (C)*: 3024
- [4] Corrie J. E. T., Green G. H., Ritchie E., Taylor W. C. (1970) *Aust. J. Chem.* **23**: 133
- [5] Pelter A., Ward R. S., Collins P., Venkateswarlu R. (1985) *J. Chem. Soc. Perkin Trans. I*: 587
- [6] Pelter A., Ward R. S., Rao E. V., Sastry K. V. (1976) *Tetrahedron* **32**: 2783
- [7] Abe F., Yahara S., Kubo K., Nonaka G., Okabe H., Nishioka I. (1974) *Chem. Pharm. Bull.* **22**: 2650
- [8] Vaquette J., Cavé A., Waterman P. G. (1979) *Planta Med.* **35**: 42
- [9] Greger H., Hofer O. (1980) *Tetrahedron* **36**: 3551
- [10] Hofer O., Schölm R. (1981) *Tetrahedron* **37**: 1181
- [11] Hofer O., Wagner U. G., Greger H. (1986) *Monatsh. Chem.* **119**: 1143
- [12] Jones W. A., Beroza M., Becker E. D. (1962) *J. Org. Chem.* **27**: 3232
- [13] Ghosal S., Banerjee S., Srivastava R. S. (1979) *Phytochemistry* **18**: 503
- [14] Hofer O., Greger H., Robien W., Werner A. (1986) *Tetrahedron* **42**: 2707
- [15] Birnecker W., Wallnöfer B., Hofer O., Greger H. (1988) *Tetrahedron* **44**: 267
- [16] Hofer O. (1986) *J. Chem. Soc. Perkin Trans. II*: 715
- [17] Willcott M. R., Lenkinski R. E., Davis R. E. (1972) *J. Amer. Chem. Soc.* **94**: 1742
- [18] Davis R. E., Willcott M. R. (1972) *J. Amer. Chem. Soc.* **94**: 1744
- [19] QCPE Program No. 136, Quantum Chemistry Program Exchange, Indiana University, Bloomington, IN 47405, USA
- [20] Hofer O., Griengl H., Nowak P. (1978) *Monatsh. Chemie* **109**: 21
- [21] Hofer O. (1976) *Topics in Stereochemistry* **9**: 111
- [22] Lewis R. B., Wenkert E. (1973) In: *Nuclear Magnetic Shift Reagents* (Sievers R. E., ed.), Academic Press, New York, London, p. 125
- [23] Erasmus C. S., Boeyens J. C. A. (1969) *Acta Cryst.* **A25**: S 162
- [24] *Handbook of Chemistry and Physics*, 63rd ed. (1982) CRC Press, Boca Raton, FL
- [25] Haas G., Hulbert P. B., Klyne W., Prelog V., Snatzke G. (1971) *Helv. Chim. Acta.* **54**: 491

- [26] Jaffé H. H., Orchin M. (1962, fifth printing 1970) Theory and Applications of Ultraviolet Spectroscopy. Wiley, New York London Sydney, pp. 114, 115
- [27] Charney E. (1979) The Molecular Basis of Optical Activity. Optical Rotatory Dispersion and Circular Dichroism. Wiley, New York, pp. 350–358 (Appendix III)
- [28] Burkert U., Allinger N. L. (1982) Molecular Mechanics (ACS Monograph 177). American Chemical Society
- [29] Quantum Chemistry Program Exchange, No. MM2(87). Indiana University, Bloomington, IN 47405, USA
- [30] Wurz G. (1989) Diplomarbeit. University of Vienna
- [31] Müller N., Falk A. (1989) Ball & Stick 2.2 for Apple Macintosh

Received April 18, 1991. Accepted May 14, 1991